Optimal Inverter Control for Voltage Phasor Matching

Kyle Brady and Calvin Choi

ME231A/EE220B Final Presentation at: https://youtu.be/PDnGOEUlUcc

***Abstract*— The large-scale adoption of distributed energy resources (DER) presents significant challenges to the operation of the power grid. Along with the difficulties that must be addressed, though, comes the possibility of recruiting these DER to provide ancillary services or accomplish high-level grid objectives. This project aims to demonstrate the effects of DER recruitment in a test case at the medium voltage "distribution" level of the grid: the goal will be the matching of a voltage phasor target at a specific node in the system. This has potential benefits for the remote control of power flow, which would be extremely useful in grid reconfiguration or repair. For this project, we test an optimal controller that both recruits DER and manages the charging/discharging of a storage battery while attempting to match a phasor target over a one-hour horizon.**

I. Background

Recent years have seen a large influx of distributed energy resources (DERs) at the medium-voltage (a.k.a. distribution) level of the electric grid. This has been driven by greater adoption of home solar systems (generally abbreviated PV, for photovoltaics) by both residential and commercial customers. As a result, the operators of distribution feeders have had to contend with the introduction of large generation uncertainties (PV forecasts, while generally good, are not foolproof) and the potential for "reverse" power flow from customers to utility. These previously unknown phenomena cause serious challenges for legacy distribution equipment and operation strategies, and much research is directed at safely accommodating expected future PV growth on our present-day grid.

Along with the difficulties presented by increasing amounts of DER, though, comes opportunity. If used correctly, DER can provide ancillary services to the grid that aid in its stability, resiliency, and efficiency of operation.

These ancillary services will be carried out most directly by the inverters that convert the direct current generated by PV units to alternating current that can be sent to the grid (inverters with a slightly different function but similar capabilities are used to connect wind turbines and other types of DER). In steady-state power system analysis, these inverters can be said to generate two "types" of power: real and reactive.

Of course, in reality there is only one type of electric power and its balance must be instantaneously satisfied at all times. The concepts of real and reactive power, though, arise as a convenient tool in dealing with alternating-current systems.

To define real and reactive power, we start by seeing that, when a power system in a steady state is viewed over time, only part of the integral of its instantaneous power exchange can be said to result in useful work. The other, generally smaller, part is simply transferred between the generator and the electric/magnetic fields of capacitive or inductive components on the grid, to be transferred back to the generator at a later point in the cycle. The useful portion of the power transferred over time is called "real" power (P), while the continuously exchanged power, which dissipates its energy in distribution lines rather than in any grid-connected devices, is called "reactive" (Q).

The real and reactive power are related to the voltages of a distribution feeder, which can be considered a network of nodes (at which customers and their power demands are located) and lines, through the power flow equations (shown here for a single phase, but treated in the optimization program as a set of three phases ABC):

$$P_i = \sum_{k\sim i} |V_i||V_k|(G_{ik}cos\theta_{ik} + B_{ik}sin\theta_{ik})$$

$$Q_i = \sum_{k\sim i} |V_i||V_k|(G_{ik}sin\theta_{ik} - B_{ik}cos\theta_{ik})$$

$$V_{slack} = 1\angle 0^\circ$$

$$\theta_{ik} = \theta_i - \theta_k$$

The three-phase voltages at node i in the feeder are specified in terms of sets of three phasors, i.e. vectors assumed to be stationary relative to a reference frame rotating at 60Hz. These voltage phasors are denoted $|V_i|\angle\theta_i$. As for the rest of the notation, $G_{ik} + jB_{ik}$ is the admittance of the line connecting nodes i and k, P_i and Q_i are the real and reactive powers consumed at node i, and the slack bus $V_{slack} = 1\angle 0$ is defined as a reference voltage for the purposes of numerically solving these equations.

Finally, although they do not appear in the equations above, u_i and v_i will represent the collective real and reactive power dispatch of all DER connected at node i. Through intelligent control of that real and reactive power dispatch, the voltage throughout the system can be influenced.

II. The Optimal DER Controller

There are many possible motivations for designing a DER dispatch controller to alter the voltage profile of a feeder: maintaining all nodes within minimum and maximum allowable voltage bands, ensuring that the system stays in a stable configuration, etc. Our controller will focus on reference tracking; attempting to match a voltage phasor target at a performance node in the system over time.

An interesting potential use case for voltage reference tracking is found on feeders that can be operated as microgrids, or self-contained power islands. Grid-tied microgrids are generally connected to the utility's network at the distribution

level, but also have the capability to disconnect and run under their own power. In order for disconnection/reconnection of a microgrid to happen, though, there must be very little voltage difference between the two sides of the switch that connects them to the grid, otherwise activating the switch will cause electric arcing that could damage equipment. The ability to dispatch DER so as to cause the voltage on one side of the switch to track the voltage on the other, then, is a means of ensuring that the switch will be able to open or close at any point in time – a critical capability if a microgrid is to be able to make split-second connection decisions in response to disturbances on the grid.

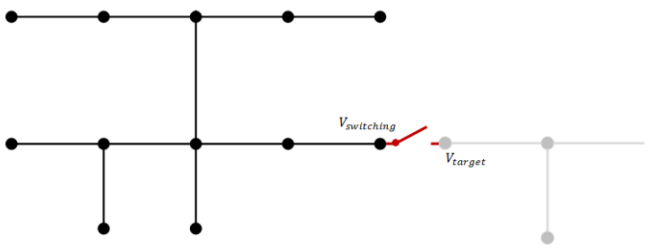

Fig. 1. A microgrid (black) connected to a distribution feeder (grey) over whose voltages it has no control. $V_{switching}$ and V_{target} would need to be very close if the grid-connection swtich were to be safely closed.

Our optimal voltage-reference-tracking DER dispatcher is built using code developed by Dan Arnold and Michael Sankur, of Berkeley's ME Department and LBNL [1]. Their work focused on the recruitment of DER to balance the magnitudes of voltage phasors on each of the three phases present at each node (excepting nodes where fewer than three phases were connected). Acting over a single time step, their program solves the optimization problem:

$$\min_{z} \sum_{i \in 3\phi} (|V|_{Ai} - |V|_{Bi})^2 + (|V|_{Ai} - |V|_{Ci})^2 + (|V|_{Bi} - |V|_{Ci})^2$$

where $z = \left[|V|^{2T}\ \theta^T\ P^T\ Q^T\ u^T\ v^T\right]$ is a set of vector variables motivated by a linearized version of the power flow equations from the previous section. This particular linearization, which involves the squares of all nodal voltage phasors, is called the LinDistFlow equations, based on the DistFlow reformulation of the power flow equations, which was developed in the 1980s [2]. The DistFlow equations become linear equations when power losses in distribution lines are neglected, thus allowing them to be included as constraints in an optimization problem. Other constraints used in this problem include Kirchhoff's laws, which are translated into sets of linear equations, and inequalities related to utility operating policies (namely the maintenance of voltages within acceptable limits.

Our work for this project expands Arnold and Sankur's program by changing their optimization script from a single-step program to a multi-step program with dynamics. By adding a model of energy storage to the network, we have added memory to the system and gained the ability to determine whether a given battery + DER configuration has the ability to carry out voltage tracking and, if so, for what length of time.

The first major change that we needed to make to adapt Arnold and Sankur's code was to change the definition of z to include multiple time steps. As a result (and with a slight abuse of notation for clarity), z should now be considered an expanded vector related to the original z defined above as $z^T = [z^{1T}\ z^{2T}\ \ldots\ z^{nT}]$, where the superscript designates the time step.

The change to the objective function in transforming Arnold and Sankur's code into ours was very straightforward. It simply involved replacing the original expression above with:

$$\min_{u,v} (|V|_{Aswitching} - |V|_{Atarget})^2 + (|V|_{Bswitching} - |V|_{Btarget})^2 + (|V|_{Cswitching} - |V|_{Ctarget})^2 + (\theta_{Aswitching} - \theta_{Atarget})^2 + (\theta_{Bswitching} - \theta_{Btarget})^2 + (\theta_{Cswitching} - \theta_{Ctarget})^2$$

Updating the constraints attached to the objective function, though, was much more difficult. The LinDistFlow equations, which related nodal voltage magnitudes and angles to power flows on the lines themselves, were able to remain unchanged, but the Kirchhoff current balance equations at each node had to be updated to include battery charge/discharge. With the further expansion to z by adding additional nodal variables X^n: the state of charge of all batteries at timestep n, xu^n: the real power consumed by the batteries at timestep n, and xv^n: the reactive power consumed by all batteries at timestep n, the Kirchhoff constraints became (we will not include the superscript here, but this constraint as written should be considered to hold at a single timestep):

$$\sum_{k \sim i} P_{ki} = xu_i + u_i + customer\ demand_i$$

$$\sum_{k \sim i} Q_{ki} = xu_i + v_i + customer\ reactive\ demand_i$$

The other major adjustment to the constraints was the addition of linkages between the battery state of charge and charging/discharging across time steps, namely:

$$X_i^n = X_i^{n-1} + xu_i^{n-1}$$

New inequality constraints enforced limits on the maximum energy stored in a given battery, as well as its maximum charging/discharging rate. Those constraints were fairly straightforward, though, and so the equations will not be included here (they can be found summarized in our project presentation video).

Simulation and Results

We tested our algorithm on a commonly used unbalanced feeder model, the IEEE 13-node feeder. That feeder generally includes a transformer and an internal switch, which we removed for the purposes of proving this algorithm.

The feeder has a standard set of load data, which specifies customer demand at each node for a single time step. We called these values our maximum customer demand, and then used an

averaged set of residential power data to define an hour-long time series normalized to that maximum. The residential data was provided by Pecan St. Inc., a organization based in Texas that has made a comprehensive smart grid dataset available to academic researchers.

We define our maximum PV capacity as a "penetration level," or a fraction of the maximum customer demand on a feeder that can be satisfied by the maximum output of all system-connected PV panels. We test PV penetration levels of 50% and 100% in our simulation. Time series data for a given level of PV penetration is generated with the help of a PV production dataset produced by NREL, an hour's worth of which was normalized to the maximum PV capacity defined by our penetration level. (Our project presentation has a visualization of this dataset).

Maximum storage capacity for our model was defined to be one third of the total feeder demand over the course of the hour. All storage was located at the performance node, simulating a large, utility-owned battery. Its maximum charging/discharging rate was set to be one tenth of its maximum storage capacity.

With those parameters, we ran our model and found that the 50% and 100% levels of solar penetration gave us some very different results. Though both levels of PV penetration were very successful at their voltage reference tracking task, at the 50% level we see that the battery slowly discharges over the course of our hour-long window. At the 100% level, we see that the battery is able to essentially maintain its full charge over the window, only occasionally discharging to respond to a time step with low solar production and high demand. In this case, it appears that our feeder could be run at net zero power export indefinitely, and be permanently ready to island.

While this may seem like an intuitive result (of course you need to have enough internal power generation to satisfy demand if you plan to continuously maintain a zero power flow into your system), it is actually very uncertain that a matching of PV generation and local demand could successfully run as a microgrid in this configuration. Because PV and load are both extremely variable, and because the interactions between inverter generation and voltage are complicated and nonlinear, this is an interesting and gratifying result.

a.

REFERENCES

[1] D.B. Arnold, M. Sankur, R. Dobbe, K. Brady, D. S. Callaway and A. Von Meier, "Optimal dispatch of reactive power for voltage regulation and balancing in unbalanced distribution systems," *2016 IEEE Power and Energy Society General Meeting (PESGM)*, Boston, MA, 2016, pp. 1-5.

[2] M. Baran and F. F. Wu, "Optimal sizing of capacitors placed on a radial distribution system," in *IEEE Transactions on Power Delivery*, vol. 4, no. 1, pp. 735-743, Jan 1989

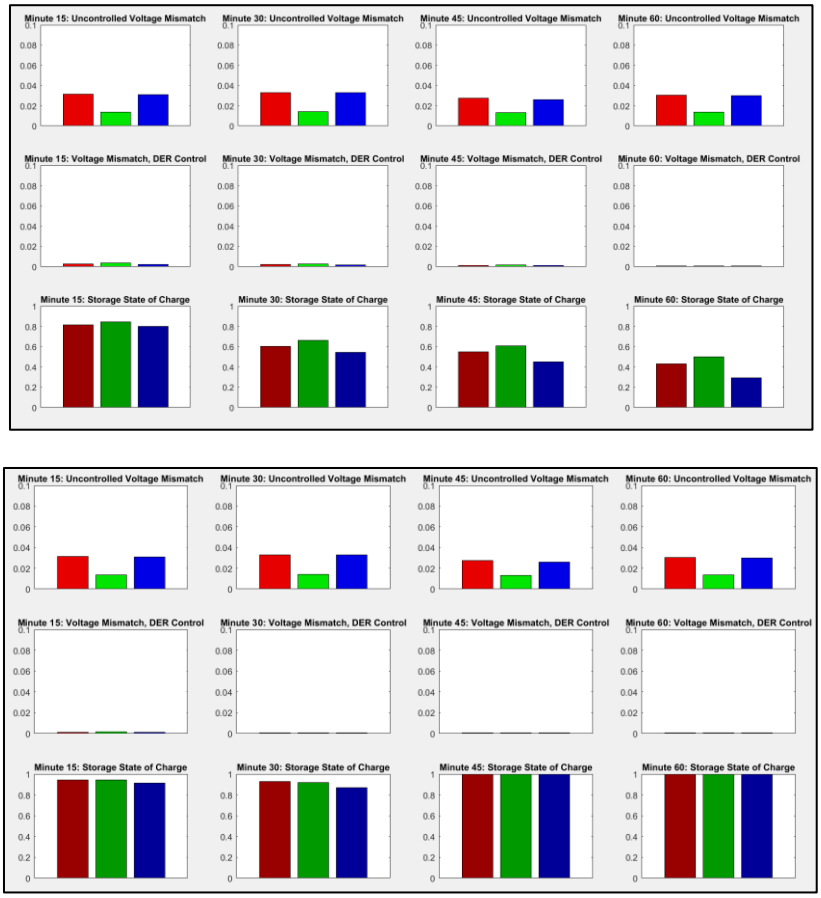

Fig. 2. The results of our simulation for 50% PV penetration (top) and 100% penetration (bottom). In each figure, the first two rows display the total vector error (TVE) in matching our phasor target. The top row shows the TVE for the case in which DER control is not active, and the middle shows the effects of our controller. The bottom row displays the state of charge of the battery. All charts display results for the system in terms of phases; the red, green, and blue bars represent phases A, B and C, respectively.